PHYSICAL REVIEW C VOLUME 54, NUMBER 2 AUGUST 1996

Effects of systematic errors in analyses of nuclear scattering data

M. T. Bennett, C. Steward, K. Amos, and L. J. Allen
School of Physics, University of Melbourne, Parkville, Victoria 3052, Australia
(Received 10 July 1995)

The effects of systematic errors in elastic scattering differential cross-section data upon the assessment of quality fits to that data have been studied. First, to estimate the probability of any unknown systematic errors, select, typical, sets of data have been processed using the method of generalized cross validation; a method based upon the premise that any data set should satisfy an optimal smoothness criterion. Specified systematic errors should also be taken into account when high quality fits to data are sought. We have considered such effects due to the finite angular resolution associated with the data in some quite exceptional, heavy ion scattering data sets. Allowing angle shifting of the measured values gave new data sets that are very smooth. Furthermore, when such allowances for systematic errors are so taken into account, reasonable, but not necessarily statistically significant, fits to the original data sets can become so. Therefore, they can be plausible candidates for the ''physical'' descriptions of the scattering processes. In another case, the S function that provided a statistically significant fit to data, upon allowance for angle variation, became overdetermined. A far simpler S function form could then be found to describe the scattering process. The S functions so obtained have been used in a fixed energy inverse scattering study to specify effective, local, Schrödinger potentials for the collisions. An error analysis has been performed on the results to specify confidence levels for those interactions. [S0556-2813(96)01707-4]

PACS number(s): 25.70.Bc, 02.60.Ed, 24.10.−i, 25.40.Cm

I. INTRODUCTION

In recent years, fixed energy inverse scattering methods [1] have proved interesting means of analyzing experimental elastic scattering data [2–6]. The aim of such methods is to determine an effective interaction acting between colliding quantal systems, starting from a set of S functions that have been obtained by fitting data; differential cross-section data usually. The quality and extent of data is crucial in determining not only these associated S functions, but also the shapes and strengths of the inversion potentials so obtained [7]. However, these qualifications are not restricted to just inverse scattering methods. They can have a pronounced influence on the results of phenomenological model searches [8] as well. Hence, we are interested in methods of smoothing experimental data so that the contributions of nonstatistical errors (known or unknown) may be minimized.

In the treatment of unknown systematic errors, spline techniques have had a long history (see Ref. [9] and references therein), and are particularly suitable for adapting to specific problems. In addition, splining software is readily available in either commercial packages, or in the public domain on the internet. One such method is that of generalized cross validation (GCV) [9] in which only the spatial coordinates and statistical information on each data point are used to determine a tradeoff between goodness of fit and smoothness of solution. There are other methods, notably kriging [10], which may be superior in smoothing certain kinds of data sets, including highly clustered ones, but we restrict ourselves to GCV in this study. In this scheme, no direct, *a priori* knowledge of any possible systematic errors is used so that this approach is quite different to those smoothing methods for which, *a priori*, the magnitudes of the systematic errors are assumed to be known. The second part of our analyses deals with a smoothing procedure of the latter kind; i.e., with the the specified values of the angular resolution with differential cross-section data on heavy ion reactions. The results of this known error consideration we designate as angle smoothed data sets.

Note that even if the best, optimally smooth data set has been found, either from the original data being of exceptional quality or after application of smoothing techniques such as the GCV, there may still exist numerous ambiguities with analyses (e.g., phase shift analyses) of that data set. Only a statistically significant fit (i.e., one for which the chi square per degree of freedom, χ^2/F, is near 1) allows ''meaningful'' conclusions about the physics of the scattering process to be contemplated for that data and for that particular search process. But by that alone, one does not have confirmation of validity of any conclusions reached since there can be more than one specification meeting the significance criterion. The addition of *a priori* physical information may help to delineate between such equivalent results, but that may also serve to prejudice in favor of certain phenomena at the expense of the true physics unless an appropriate weighting of the effects of that *a priori* input is made. However, both the GCV and angle smoothing techniques do help to ascertain the success of an analysis with more certainty. They may simultaneously help in the definition of the limits of current theoretical models of quantal scattering (nuclear in particular), by providing a more ''realistic'' data set in that the content of nonstatistical information has been minimized. In any case, as will be shown, it is important that known systematic error in the form of finite angular resolution should always be included in high quality analyses of cross-section data.

The method of generalized cross validation is described in Sec. II. In Sec. III, details of the calculations are shown and the results are discussed in Sec. IV.

Three cases are studied, namely the differential cross-section data sets from the elastic scattering of 200 MeV protons from ^{12}C [11], of 350 MeV ^{16}O-^{16}O scattering [12], and of 288.6 MeV ^{12}C-^{12}C scattering [13]. Past analyses of the first two data sets (Refs. [14,5]), for the proton and ^{16}O scatterings, respectively, extracted effective interactions by using fixed energy inverse scattering theory, notably of the Lipperheide-Fiedeldey (LF) type [15]. In the study of proton scattering, an error analysis of the result was also made.

Thus herein we report on the results we have obtained using LF fixed energy inverse scattering theories to specify new candidate heavy ion interactions for the ^{16}O-^{16}O collision (given that there is now a very extensive data set available) and an effective Schrödinger interaction for the 288.6 MeV ^{12}C-^{12}C collision. Confidence limits on both interactions have been found as well and at all radii. The theories used to effect the fixed energy inversions and to make the error analysis are reviewed in brief in Sec. V while the results are presented and discussed in Sec. VI.

Conclusions we can draw from these studies are presented in Sec. VII.

II. GENERALIZED CROSS VALIDATION AND ANGLE SMOOTHING

Smoothing splines provide ''nice'' curves with which one may smooth discrete, noisy data. A practical, effective method by which they may be used to estimate the optimum amount of smoothing of data has been specified by Craven and Wahba [9]. Their method uses generalized cross validation (GCV) to estimate the appropriate degree of smoothing and therewith prescribes a mathematical scheme to assess inherent systematic errors in the starting data set. A full account of the method has been given in Ref. [9] and so only a brief outline is presented herein.

The Craven-Wahba model considers that an n entry data set, y_i, can be specified by

$$y_i = g(t_i) + \epsilon_i, \tag{1}$$

where $g(t_i)$ are smooth polynomials and $\{\epsilon_i\}$ are random errors (white noise) for the given parametric values $t_i \in [0,1]$.

The problem one faces is to find functions f that minimize the expression

$$\frac{1}{n}\sum_{j=1}^{n} [f(t_j) - y_j]^2 + \omega \int_0^1 [f^{(m)}(u)]^2 du, \tag{2}$$

where the parameter ω controls the tradeoff between the ''roughness'' of the solution, as measured by

$$\int_0^1 [f^{(m)}(u)]^2 du, \tag{3}$$

and the infidelity to the data specified by

$$\frac{1}{n}\sum_{j=1}^{n} [f(t_j) - y_j]^2. \tag{4}$$

As an estimate of f, it is customary to start with the smoothing polynomial splines $g_{n,\omega}(u)$ of degree $2m-1$. Our calculations have been made with cubic splines, i.e., with the choice of $m=2$. The cross validation process we have used finds the optimal value for the parameter ω in a self-consistent way [9].

We have also sought a smoothing method to allow for the magnitudes of known systematic errors. For the data concerned, those are the known values of the angular resolution with the measured differential cross-section data. We have treated that information as an angle uncertainty allowing us to adjust the data set within those specified limits and have simply adjusted the identifying angles to optimally agree with the best theoretical fit we could find to the original data. The results of this known error consideration we designate as angle smoothed data sets.

III. DETAILS OF CALCULATIONS

There are diverse techniques by which generalized cross validation of a data set can be made. We have used those encapsulated in the GCV package in the (well-known) NETLIB routines that are to be found in the public domain library of computer software /pub/netlib/gcv at ftp.cs.uow.edu.au. There is also a suite of GCV subroutines available in the International Mathematics and Statistics Library (IMSL). The programs of either library generate new data sets from the input empirical ones; with the smallest adjustments possible made to any and all of the data (in magnitude but not scattering angle) so that the smoothest spline interpolates the results. To illustrate how significant the apparently small changes wrought by the GCV and/or the angle smoothing processes can be, we consider the variations that result to S functions designed to fit the data. Such a process is the first step in most fixed energy inversion analyses of scattering cross sections, and so we have chosen the rational form for the S function that is the usual initial quantity for inversion schemes of the LF type [15], whether used in semiclassical (WKB) [3,6] or fully quantal inversion [4–6] applications, namely

$$S(\lambda) = S_{\rm ref}(\lambda) \prod_{n=1}^{N} \left(\frac{\lambda^2 - \beta_n^2}{\lambda^2 - \alpha_n^2} \right), \tag{5}$$

λ being the angular momentum variable. Physical values coincide with $\lambda = l + 1/2$. In this S function, $S_{\rm ref}(\lambda)$ is a reference S function which we take as

$$S_{\rm ref}(\lambda) = e^{i\eta \ln(\lambda^2 + \lambda_c^2)}, \tag{6}$$

where η is the usual Sommerfeld parameter and λ_c is a background cutoff parameter. The complex parameters $\{\alpha_n, \beta_n\}$ have been adjusted so that we find a best fit to each data set as defined by a minimal value to the chi square per degree of freedom, χ^2/F. In our context the degree of freedom is the difference between the number of data points and the number of adjustable parameters.

IV. RESULTS OF APPLICATION OF GCV AND ANGLE SMOOTHING

We have applied these processes to two sets of heavy ion elastic scattering data taken by the experimental group at the

TABLE I. The rational function parameters that gave the fit to the 200 MeV p-^{12}C cross-section data. The background cutoff parameter, λ_c, was chosen to be 0.2. The rows labeled ''Orig'' contain the values of the parameters determined by a fit to the original data set, while those labeled ''GCV'' give the parameter values for a fit to the GCV data set.

		α_n		β_n	
		Real	Imaginary	Real	Imaginary
$n=1$	Orig	10.0131	−5.9492	1.1305	3.4212
	GCV	10.2394	−5.9830	1.6833	3.5518
$n=2$	Orig	26.8805	−42.6996	0.5574	3.0838
	GCV	26.4927	−42.5370	0.3576	2.7283
$n=3$	Orig	2.7100	−3.0292	−4.3915	3.0549
	GCV	2.6652	−3.1173	−4.4325	3.2730
$n=4$	Orig	−2.6745	−2.7727	−12.6607	11.6069
	GCV	−2.6827	−2.7197	−12.4330	11.2518
$n=5$	Orig	−4.2938	−16.6161	−22.8934	42.9272
	GCV	−2.9102	−16.0866	−23.1430	43.0483

Hahn-Meitner Institüt, Berlin and to a proton elastic scattering cross-section data set measured by Meyer *et al.* at the IUCF, Indiana.

Of those, we consider first the differential cross-section data from the elastic scattering of 200 MeV protons off of ^{12}C [11]. Next we analyze the extensive set of ^{16}O-^{16}O differential cross-section data that was taken at 350 MeV [12]; quite exceptional nuclear heavy ion data given the range of scattering angles specified. Finally we have analyzed the cross-section data from ^{12}C-^{12}C scattering at 288.6 MeV [13].

In the case of proton scattering, no information on known systematic errors was available, so only the GCV technique has been used with that data set. For the heavy ion scattering data sets however, the effect of a 0.1° uncertainty on the scattering angles also was investigated. In the diagrams depicting the cross-section data and fits, the original data sets are depicted by solid circles while the GCV sets are shown by open circles. If at any scattering angle the two sets coincide, the GCV designation (open circles) predominates. The results of angle adjustment of data are displayed in relevant diagrams by the open squares.

The fits to data are shown in full first and then in segments not only to clearly demonstrate the high quality nature of the data sets, but also to show which specific subset of data points contributes most significantly to the overall χ^2 values of any fit. Tables I – III give the relevant parameters that determine the S function for each data set, while in Table IV we have summarized the contributions to the total fit values of χ^2 from segments of the original, the cross validated, and, where relevant, the angle smoothed data sets.

A. The 200 MeV proton-^{12}C cross section

The differential cross section for p-^{12}C scattering at 200 MeV is compared with the best fit result in Fig. 1. It is shown there for the complete angular range measured in the experiment. The solid line portrays our best fit to the original data set for which we found a value of 28.8 for χ^2. Application of the GCV process gave a new data set which is barely distinguishable from the original, and an independent search for a fit to that GCV data gave an S function of form Eq. (5) and with which the χ^2 fit was 29.0. The cross section is not discernible from that shown in Fig. 1. The rational function parameters of the S functions that gave these high quality fits to both the original and GCV data sets are given in Table I. The χ^2/F values in these cases were 0.99 and 1.00, respectively; values that definitely identify the fits as statistically

TABLE II. The rational function parameters that gave the fit to the 350 MeV ^{16}O-^{16}O cross-section data. The background cutoff parameter, λ_c, was chosen to be 1.92.

	α_n		β_n	
	Real	Imaginary	Real	Imaginary
$n=1$	54.2908	−11.4607	24.0430	3.1105
$n=2$	65.7168	−20.9684	57.5211	19.9136
$n=3$	−62.5244	−20.0659	34.1675	34.7576
$n=4$	−10.3285	−2.9333	−25.9941	3.3402
$n=5$	−16.0811	−39.5517	−2.5332	2.4529
$n=6$	−28.0978	−14.5510	−41.3634	19.2387
$n=7$	−37.9825	−11.7218	−50.8647	2.7793
$n=8$	−13.6747	−10.3874	−59.4870	8.0638
$n=9$	−24.0183	−3.1871	9.7988	3.0394

TABLE III. The rational function parameters that gave the fit to the 288.6 MeV ^{12}C-^{12}C cross-section data. The background cutoff parameter, λ_c, was taken to be 1.73. The rows labeled ''Orig'' contain the values of the parameters determined by a fit to the original data set, while those labeled ''GCV'' give the parameter values for a fit to the GCV data set.

		α_n		β_n	
		Real	Imaginary	Real	Imaginary
$n=1$	Orig	27.744523	−14.389995	3.796999	9.515195
	GCV	28.317065	−14.202606	3.916821	9.520174
$n=2$	Orig	27.008218	−13.488378	−8.739953	15.988789
	GCV	27.505197	−13.372077	−8.324556	16.115838
$n=3$	Orig	−2.917832	−1.476174	−3.851786	4.834795
	GCV	−2.968014	−1.460472	−3.854648	4.867008
$n=4$	Orig	−9.831692	−6.186899	43.143690	10.541231
	GCV	−9.885386	−6.145712	43.270682	10.490968
$n=5$	Orig	−20.589188	−7.171096	−33.211045	6.013674
	GCV	−20.639399	−7.266823	−33.437661	6.486210
$n=6$	Orig	−15.227739	−27.310543	22.629528	15.792581
	GCV	−14.884547	−27.445701	22.929486	15.662967
$n=7$	Orig	−35.596499	−8.147487	−24.006946	6.267502
	GCV	−35.570996	−8.107553	−23.871387	6.444519
$n=8$	Orig	−43.939140	−8.960540	27.586294	5.983191
	GCV	−43.926832	−8.998362	28.086728	5.996632

TABLE IV. The contributions to the χ^2 and χ^2/N values from angular segments of the original differential cross-section data and of the cross validated set. The values of χ^2/F for the total results are given in brackets.

		Original data	GCV data	Angle smoothing
p-^{12}C	Angular segment	$\chi^2 : \chi^2/N$	$\chi^2 : \chi^2/N$	
	0–40	10.4 : 0.65	9.65 : 0.60	
	40–80	2.15 : 0.14	2.02 : 0.13	
	80–120	16.2 : 0.90	17.3 : 0.96	
	0 160	28.77 : 0.59	28.96: 0.59	
		(0.992)	(0.998)	
^{16}O-^{16}O	Angular segment	$\chi^2 : \chi^2/N$	$\chi^2 : \chi^2/N$	$\chi^2 : \chi^2/N$
	0– 4	326.5 : 65.3	145.9 : 29.2	8.61 : 1.72
	4 – 7	187.7 : 20.9	140.6 : 15.6	6.89 : 0.77
	7 – 10	573.3 : 22.1	426.11 : 17.0	18.7 : 0.75
	10 – 13	347.2 : 11.6	301.2 : 10.0	36.5 : 1.22
	13 – 20	131.8 : 2.69	119.3 : 2.43	7.98 : 0.16
	20 – 27	51.5 : 2.15	51.9 : 2.16	30.4 : 1.27
	27 – 34	23.0 : 1.91	22.9 : 1.91	7.13 : 0.59
	0 – 34	1641.1 : 10.6	1207.8 : 7.84	116.2 : 0.75
	0 – 75	1706.1 : 8.57	1274.7 : 6.44	150.8 : 0.76
		(10.5)	(7.86)	(0.98)
^{12}C-^{12}C	Angular segment	$\chi^2 : \chi^2/N$	$\chi^2 : \chi^2/N$	$\chi^2 : \chi^2/N$
	0–10	15.2 : 0.76	5.48 : 0.27	4.03 : 0.20
	10–15	9.87 : 0.58	6.60 : 0.39	1.80 : 0.10
	15–20	18.5 : 1.16	17.7 : 1.11	5.89 : 0.42
	20–25	12.6 : 0.84	12.6 : 0.84	7.56 : 0.47
	25–30	8.03 : 0.62	8.02 : 0.62	5.04 : 0.39
	30–35	2.08 : 0.26	2.08 : 0.26	1.64 : 0.20
	35–40	2.39 : 0.34	2.39 : 0.34	2.06 : 0.29
	0–40	68.70: 0.72	54.88 : 0.57	28.01 : 0.29
		(1.07)	(0.86)	(0.44)

significant ones. There is little to distinguish one data set from the other, and concomitantly, one calculated cross section from the other. Thus, in Fig. 2, we show the two data sets and the fit to the original data set (no difference is apparent with the fit to the GCV data even on this expanded scale) for segments of the scattering angle range, 0°–40°, 40°–80°, and 80°–120°, specifically. There is little distinction between the two data sets even on these expanded scales (remember that the GCV data takes precedence whenever the two data plots overlap). By this criterion, the original data set is optimally smooth. The similarity of the original and GCV results is emphasized by the close comparison in the cross-section segment values of the χ^2 that are given at the top of Table IV.

The modulus and phase of the rational S function that fits the original data from p-^{12}C scattering at 200 MeV are shown in Fig. 3 and in the top and bottom segments, respectively. As with the cross sections themselves, the magnitude and phase of the S function found by the fit to the GCV data are indistinguishable from those displayed in Fig. 3 on the scale given. Thus the differences in the values of the pole–zero-pair values found by the independent searches essen-

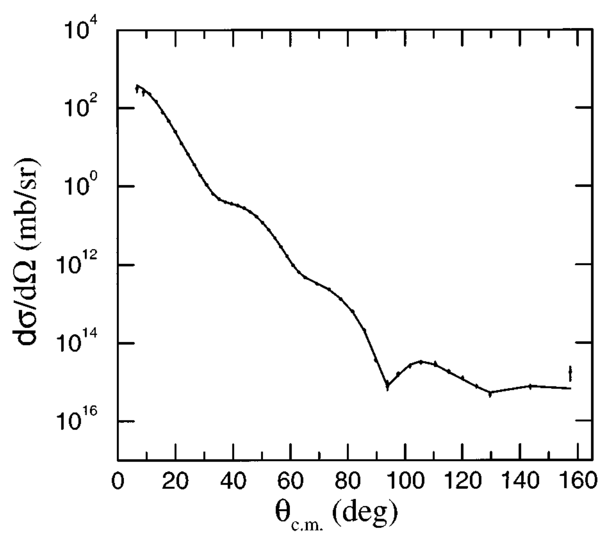

FIG. 1. The differential cross section for p-^{12}C scattering at 200 MeV. The solid line corresponds to the χ^2=28.8 fit to the original data set.

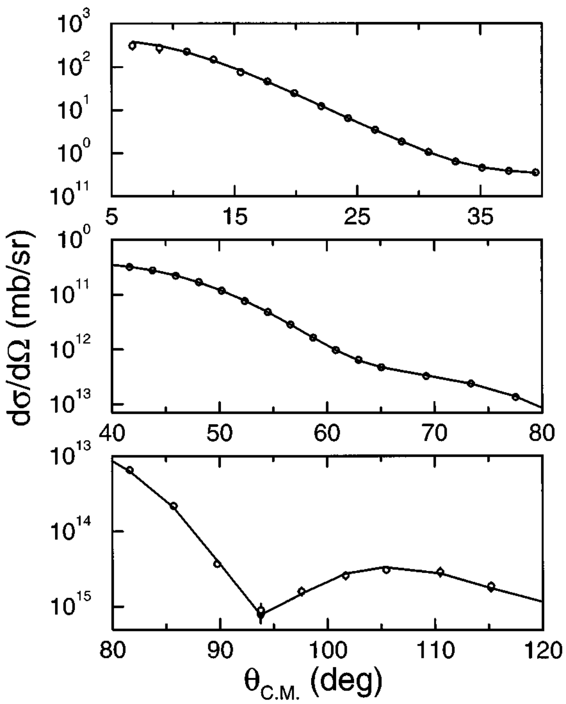

FIG. 2. The differential cross sections for 200 MeV protons elastically scattered from ^{12}C shown by segments. The solid circles correspond to the original data set, and the open circles (taking precedence where there is overlap) correspond to the GCV data set. The solid line corresponds to the $\chi^2=28.8$ fit to the original data set.

tially reflect only the ambiguity in the parametric form for the S function.

The absorption attribute in the S function is weak with the modulus being quite large save for the very smallest angular momentum values, and not very structured. The associated scattering potential will have a smooth Woods-Saxon-like form [14]. We are cognizant of the need for spin-orbit interactions in proton-nuclei optical potentials, and so need S functions that are functions of the total angular momentum as well, viz., $S(\lambda,j)\equiv S^{(\pm)}(\lambda)$. To some extent, however, the cross sections reflect the average of the two sets.

B. The 350 MeV ^{16}O-^{16}O cross section

The complete measured differential cross section for ^{16}O-^{16}O scattering at 350 MeV and the best fit we could find using rational function forms of the S functions are compared in Fig. 4. Using the parameters given in Table II we obtained the cross section as displayed by the solid curve in Fig. 4 and with which we found a fit to the original data set with a (total) χ^2 value of 1706.1. As for the p-^{12}C case, the differential cross section results for the GCV analysis, both the data set and the cross-section fit, are not displayed in Fig. 4. On the scale of this diagram, differences between the GCV and original results are not apparent. The associated values of χ^2/F are not as small as would be desired in these cases, being 10.5 and 7.9, respectively. We note that the values of chi square per data point are 8.6 and 6.4, respectively. That fit criterion has been used by others in analyses of this and other heavy ion scattering data, but it is more relevant to take the number of free parameters into consideration. Studies that effectively use every radial value of a model interaction potential as adjustable may find reasonable fits to scattering data according to the determined value of chi square per data point, χ^2/N, but run the risk of having meaningless (even negative) values of χ^2/F. As goes the old adage: ''*With enough free parameters, one can fit an elephant!*'' But our search with the GCV data has been constrained. First, we sought pole–zero-pair fit values that we could use with the inversion methods to specify an ^{16}O-^{16}O inversion potential. The result is a set of pole–zero-pair parameter values very close to the original set listed in Table II. If we allowed the search to be unfettered then we could find a much better fit to the GCV data set. A value $\sim$2.5 for the χ^2/F can be found but the result cannot be inverted with our present methods as the pole-zero pairs have very small imaginary values. However, we have not pursued those S functions further for an-

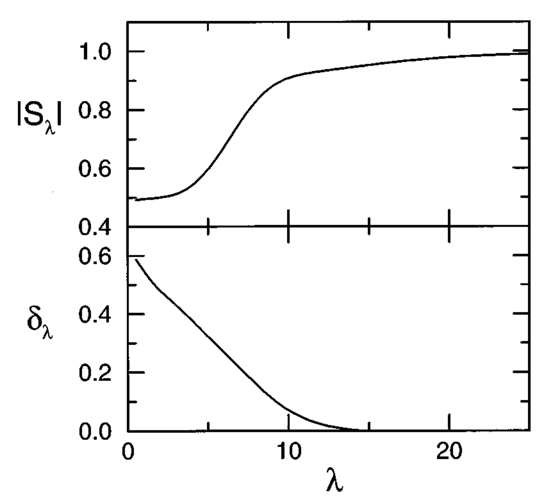

FIG. 3. The moduli (top) and phases (bottom and in rad) of the rational S function with which the original data set for p-^{12}C scattering at 200 MeV was fitted with a χ^2 of 28.8.

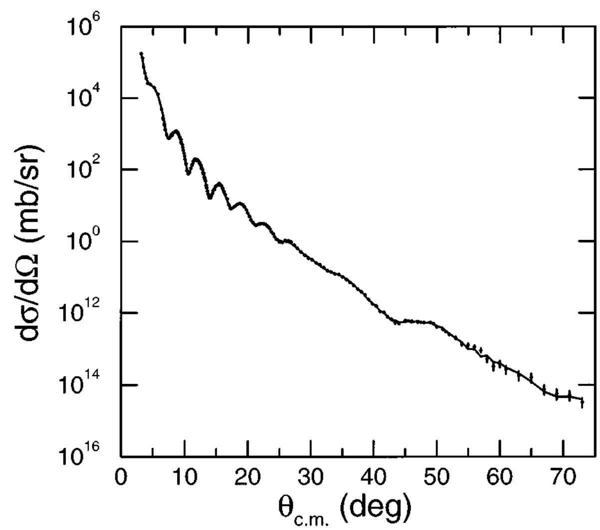

FIG. 4. The differential cross section for ^{16}O-^{16}O scattering at 350 MeV. The solid line corresponds to the $\chi^2=1706.1$ fit to the original data.

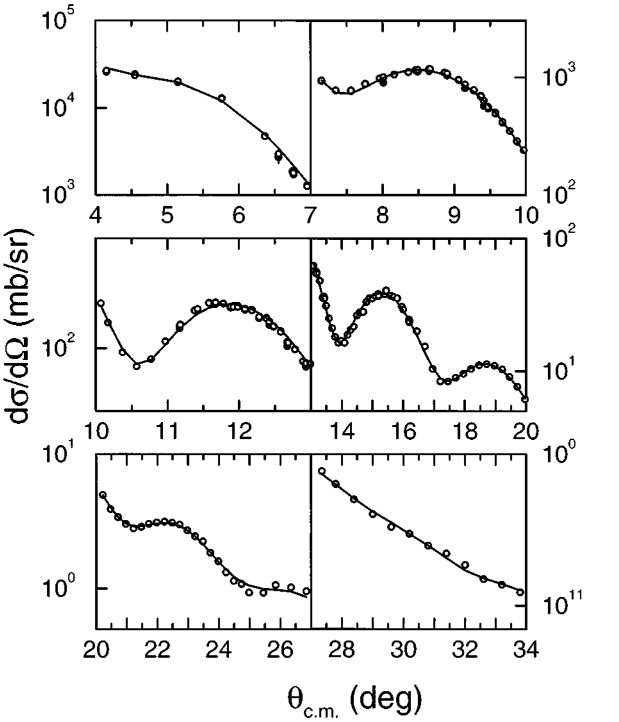

FIG. 5. The differential cross sections for ^{16}O-^{16}O scattering at 350 MeV for diverse scattering angle segments. The solid circles show the original data set, and the open circles give the GCV results (taking precedence where there is overlap between the two). The curve displays the fit with χ^2 of 1706.1 to the complete data set.

other reason as well. As will be shown, angle smoothing of the data has a profound effect.

The data spans 10 orders of magnitude and so it is not surprising that with the complete result plotted in Fig. 4 there is no distinction between the original and GCV data sets. Likewise on this scale one would consider the fits to data to be near perfect. But quite a different view results when the data are plotted in angular segments and on expanded scales. The angular segments 4°–7°, 7°–10°, 10°–13°, 13°–20°, 20°–27°, and 27°–34° are displayed in Fig. 5, where we have included both the original (solid circles) and the GCV data (open circles) as well as the fit to the original data (solid curve). Clearly GCV smoothing adjusts many of the data points in the small angle regions (to 15° in particular) and is the prime reason why the fit to the GCV data with essentially the same S function that ''best fit'' the original data gave the improved value of χ^2/F.

The modulus and phase of the rational S function we have found from the fit to the original data set from ^{16}O-^{16}O scattering at 350 MeV, are displayed in Fig. 6. Note that the phase is plotted modulo π to keep the vertical scale of the diagram small. This S function has much more structure than that given before (for the p-^{12}C scattering). Also as the extensive data set spans 10 orders of magnitude the fits are extremely sensitive to details of the S functions. Therefore, although both the original and GCV data fit S functions are essentially the same, small numerical differences between the two have in part been responsible for the difference in χ^2/F values found. It was necessary to carry at least six-figure accuracy with each value of $S_l(k)$ when the fitting

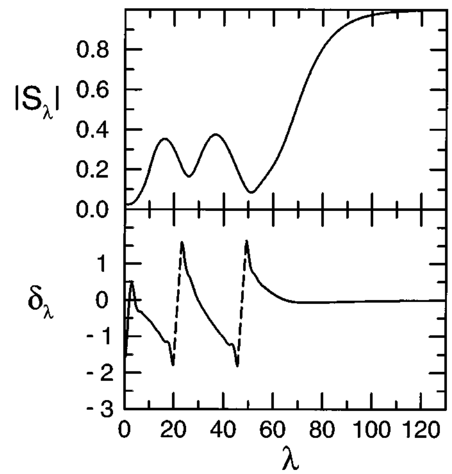

FIG. 6. The moduli (top) and phases (bottom and in rad) of the rational S functions with which a fit measured by $\chi^2 = 1706.1$ is found to the cross section from ^{16}O-^{16}O scattering at 350 MeV.

process was used to ensure that the resultant cross section was indeed accurately calculated, especially at large angles. Hence the number of significant figures in the tabulation of the pole-zero pairs of parameters in Table II. Only with such detailed S functions could the original and GCV data sets (of 198 points) be fit; and even then with less than satisfactory values of χ^2/F.

But there is a 0.1° spread in the angles at which measurements for the 350 MeV ^{16}O-^{16}O cross section were made [12]. As noted previously, we have treated that information as an angle uncertainty allowing us to adjust the data set within specified limits to find an optimal agreement with the best theoretical fit we could find to the original data. That fit, having χ^2/F of 10.5, is displayed in Figs. 4 and 5. This new data set is shown in the segment plots, Fig. 7, by the open squares. We stress that the shifts never take a data point outside of the quoted 0.1° limit. The χ^2/F fit to the new, angle smoothed data set is 0.98; an order of magnitude improvement upon the original 10.5 value. Table IV shows the contribution to χ^2 for various angular ranges. It can be seen that the bulk of the total χ^2 comes from comparison at the forward scattering angles. Contributions to the total χ^2 from the large scattering angles have a negligible effect. In fact, the results for angles below 15° account for approximately 90% of the total χ^2 for the best fit ($\chi^2/F = 10.5$) to the original data. When we applied the generalized cross validation to this new, smoothed data set, no discernible difference results. So far as total χ^2 is concerned, the original ''best fit'' theoretical cross section gave a value of 150.8 when taken against the new smoothed data, while it gave 151.2 against the GCV data set found by using the smoothed data as input. As noted previously by Brunger *et al.* [16], with data sets of such extent, and when quality fits to that data set are to be specified, the analyses must allow for the angle resolution quoted for the experiment. In the present case that made an order of magnitude difference; and an order that changed the result of an analysis to be statistically significant.

C. The 288.6 MeV ^{12}C-^{12}C cross-section data

The complete measured differential cross section for ^{12}C-^{12}C scattering at 288.6 MeV is displayed in Fig. 8. The

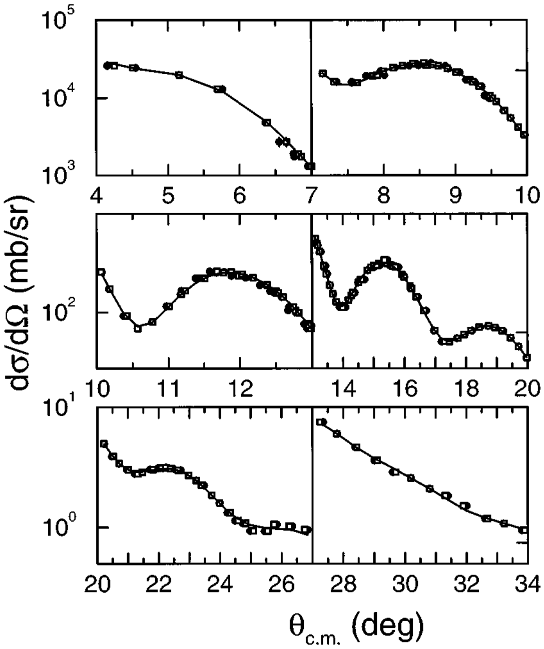

FIG. 7. The differential cross sections for ^{16}O-^{16}O scattering at 350 MeV for diverse scattering angle segments. The solid circles show the original data set, and the open squares give the angle smoothed set (taking precedence where there is overlap between the two). The curve displays the fit with χ^2 of 1706.1 to the complete data set.

GCV data set (and calculated result) is not displayed as, on this scale, it is inseparable from the original data set (and result). Our best fit to the measured cross section is displayed on the same figure as a solid line. This fit was obtained using the (''Orig'') parameters of Table III and the relevant value of (total) χ^2 is 68.7. The GCV rational function parameters of Table III led to a fit to the GCV data set and with a χ^2 value of 54.9. These correspond to χ^2/F values of 1.07 and 0.86, respectively, so that both results are statistically significant. However, as the value of χ^2/F for the GCV result is just less than 1, it may be argued that for this, the S function

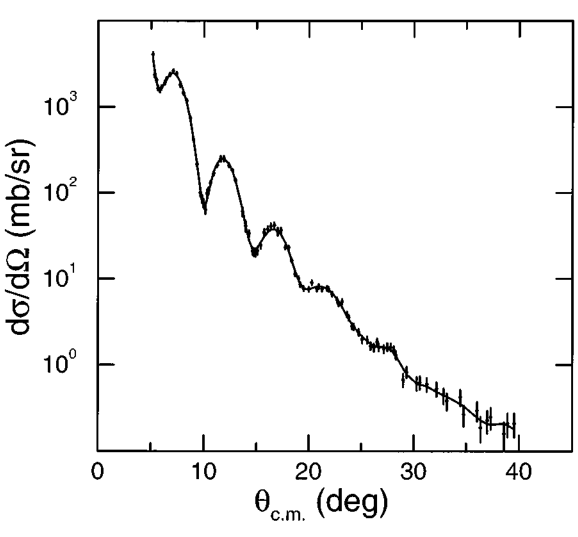

FIG. 8. The differential cross section data for ^{12}C-^{12}C scattering at 288.6 MeV compared with the fit corresponding to $\chi^2=68.7$.

TABLE V. The quality of fit to angle smoothed 288.6 MeV ^{12}C-^{12}C data found by using n-pole–zero pairs to describe an S function of the form Eq. (5), and under the constraint that those S functions can be inverted.

n	χ^2	χ^2/F
8	28.01	0.44
6	35.61	0.49
5	64.46	0.85
4	85.12	1.06

is slightly overparametrized. Therefore, we have the interesting case of a statistically significant result, originally described by an appropriate number of parameters, being perhaps slightly overdetermined once a smoothness criterion is introduced via the GCV procedure. Given that the S function was slightly overparametrized when fitting this GCV data, we deleted the largest valued pole and zero (α_8 and β_4) from the eight given in Table III and undertook another search for a seven-pole–zero-pair S function with $\chi^2/F\sim 1$. A successful fit to the GCV data was found with $\chi^2=79.8$ and $\chi^2/F=1.17$. Therefore, the number of parameters required to find a statistically significant fit has been reduced by four — a reduction of 12.5%.

To take the principle of smoothness one step further, we also applied the 0.1° uncertainty with the scattering angles, again by allowing the experimental data to be moved anywhere within that $\pm 0.1°$ angular range to result in the most optimally smooth new data set. Accounting for angular resolution in that way, the χ^2/F of our best result decreased from 1.07 to 0.44; a value notably less than one. A breakdown of these fits for various 5° angular ranges is given in Table IV. Evidently at forward scattering angles the differential cross section is most affected by these considerations of systematic errors. The results at angles less than about 25° particularly are affected. In the angular range 5°–10° the value of (total) χ^2 is reduced by more than a factor of 3 once $\Delta\theta_{c.m.}$ is taken into account while in the range 10°–15°, the χ^2 is reduced by a factor of 6. Once again a statistically significant result has become overdetermined by taking into account a smoothness requirement of the data. The S function which gave a good description to the original data with eight-pole–zero pairs is now clearly overparametrized. As above with the GCV data case, we sought to find a simpler S function, i.e., one specified by fewer pairs but with a statistically significant fit to the (angle smoothed) data set. Therefore, we reduced the set of $\{\alpha_n,\beta_n\}$ progressively seeking to have a fit with statistical significance while retaining a form that can be inverted. The results of our searches are displayed in Table V, and therein ''n'' denotes the number of pole-zero pairs employed. Starting with the $n=8$ pair S function which fitted the angle smoothed data with $\chi^2/F=0.44$, we were able to reduce the parametrized S function to one with $n=4$ pairs and still have a fit to the angle smoothed data with $\chi^2/F=1.06$; a value essentially identical to that of the eight-pair fit to the original data.

However, if we revert to using the original data, this simpler ($n=4$) S function does not give a cross section with a χ^2/F as an alternative minimum to the original (eight-pair) result. But, by using that four-pair S function to initiate a

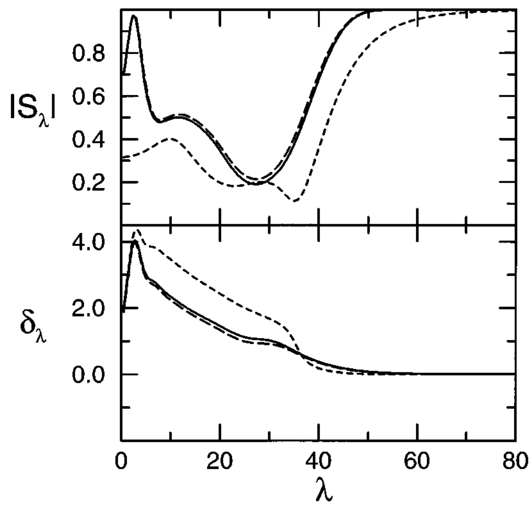

FIG. 9. The moduli (top) and phases (bottom and in rad) of the rational S functions for ^{12}C-^{12}C scattering at 288.6 MeV. The solid line is the S function found from the fit to the original data set, the long-dashed line to that from a fit to the GCV data set, and the short-dashed line is that of the four-pair S function described in the text.

new search against the original data does. Starting from a (total) χ^2 value of 127.4 ($\chi^2/F=1.59$), a minimum was found with $\chi^2=96.21$ and $\chi^2/F=1.20$. Recall that our original result discussed above involved eight-pole–zero pairs specifying an S function that gave a fit to original data with $\chi^2/F=1.07$. The success of this procedure [in finding the much simpler (four-pair) S function fit to the original data] is significant. Without having a good starting set, it was impossible for us to find this specific minimum. It is a very sharp minimum in the parameter space. Thus angle smoothing the data not only allowed us to find a much simpler S function to fit that angle smoothed data with statistical significance, but also it has proved to be a scheme to obtain a (simpler) S function with which to fit the original data with statistical significance.

The moduli and phases of three rational S functions that were found to describe ^{12}C-^{12}C scattering at 288.6 MeV are shown in Fig. 9 in the top and bottom panels, respectively. The solid line indicates results obtained using the original data set while the long-dashed line shows those where the GCV data set has been employed in our fitting procedure. There are discernible differences between those two results: the GCV result differs from the original result in that the curve for the modulus (phase) is above (below) that for the original result, albeit only slightly. These slight differences are reflected in the parameters of the S functions, the pole-zero pairs $\{\alpha_n,\beta_n\}$, which are listed in Table III. But the third result, displayed by the small-dashed line in Fig. 9, is the optimal four-pair S function with which the fit to the original data gave a χ^2/F value of 1.20. It is noticeably different from the other two displayed having a broader well-like character to the modulus of the S function and a slightly larger phase for the most important partial waves. The potentials obtained by inversion of these S functions will be different. For completeness we give the starting and final four-pair S function parameter values in Table VI.

TABLE VI. The result of searching for the optimal four-pole–zero-pair S function which can be inverted and best fits the measured 288 MeV ^{12}C-^{12}C scattering data. The set designated ‘‘Start’’ is that found by using the smoothing processes described in the text and the search result is identified as ‘‘Best.’’ The χ^2/F reduces from 1.6 to 1.2 with this search.

		α_n		β_n	
		Real	Imaginary	Real	Imaginary
$n=1$	Start	−11.3410	−6.0709	−8.2442	12.0089
	Best	−10.7096	−6.0241	−7.0200	11.0099
$n=2$	Start	−12.2498	−29.1349	24.7122	18.7739
	Best	−12.3568	−28.9806	23.0092	20.3216
$n=3$	Start	−36.5267	−9.9735	−20.8193	6.5200
	Best	−35.7060	−10.1739	−21.7706	7.0669
$n=4$	Start	37.1609	−15.0033	−34.8925	1.8520
	Best	37.3347	−15.0776	−35.4157	1.8271

V. INVERSION POTENTIALS FROM THE SCATTERING DATA

There are a number of inverse scattering theories for fixed energy data (such as differential cross sections) as may be found in the review [1] and elsewhere. Our interest is with those of the LF type for which the S functions described above are the basic input. Herein we consider both the WKB approximation LF scheme as well as a fully quantal one. A brief specification of both these schemes are given next for completeness and to define quantities that will be discussed subsequently.

In the WKB approximation [3], the phase shift function relates to a quasipotential, $Q(\sigma)$, by

$$\delta(\lambda,k)=-\frac{\mu}{\hbar^2k^2}\int_\lambda^\infty\frac{Q(\sigma)}{\sqrt{\sigma^2-\lambda^2}}\sigma d\sigma, \tag{7}$$

and which, by an Abel integral transform [1] gives the quasipotential as

$$Q(\sigma)=\frac{4E}{\pi}\frac{1}{\sigma}\frac{d}{d\sigma}\left(\int_\sigma^\infty\frac{\delta(\lambda,k)}{\sqrt{\lambda^2-\sigma^2}}\lambda d\lambda\right). \tag{8}$$

The scattering potential then is specified by the Sabatier transform,

$$V(\rho)=E\left[1-\exp\left(-\frac{Q(\sigma)}{E}\right)\right], \tag{9}$$

so long as there is a one-to-one correspondence between ρ and the dimensionless variable, σ, via the transcendental equation,

$$\rho=kr=\sigma\exp\left(\frac{Q(\sigma)}{2E}\right). \tag{10}$$

To apply the WKB fixed energy inversion scheme, it is particularly useful to recast the (fixed energy) phase shift function in the form

$$\delta(\lambda,k)=\frac{1}{2i}\sum_{n=1}^{N}\left[\ln(\lambda^2-\beta_n^2)-\ln(\lambda^2-\alpha_n^2)\right], \qquad (11)$$

for which the S function has the rational form given previously in Eq. (5), as then the quasipotential is analytic. Explicitly that quasipotential is

$$Q(\sigma)=\frac{2E\eta}{\sqrt{\sigma^2+\lambda_c^2}}+2iE\sum_{n=1}^{N}\left[\frac{1}{\sqrt{\sigma^2-\alpha_n^2}}-\frac{1}{\sqrt{\sigma^2-\beta_n^2}}\right]. \qquad (12)$$

The same rational function form for the S function can be used to effect a fully quantal inversion of the data by one of the set of LF methods. In the simplest of those schemes, the so-called rational scheme, the inversion potential is derived by the iteration

$$V_n(r)=V_{n-1}(r)+\Delta^{(n)}(r), \qquad (13)$$

where, with $V_0(r)$ being the potential associated with the chosen reference S function, $S_0(\lambda)$, the final inversion potential is $V_N(r)$. For each pole-zero pair in the N set, the increment is given in terms of the Jost solutions from the interaction of the preceding iterate, $f_\lambda^{(\pm)}(r)$, by

$$\Delta^{(n)}(r)=\frac{2i}{r}(\beta_n^2-\alpha_n^2)\frac{d}{dr}\left(\frac{r}{L_{\beta_n}^{(-)}(r)+L_{\alpha_n}^{(+)}(r)}\right), \qquad (14)$$

where the logarithmic derivatives are

$$L_\lambda^{(\pm)}(r)=\pm\left(\frac{(d/dr)f_\lambda^{(\pm)}(r)}{f_\lambda^{(\pm)}(r)}\right). \qquad (15)$$

But there is a restriction for stable solutions that the poles and zeros of the S function must lie in the first and fourth quadrants of the complex λ plane. In finding optimal fits to scattering data, that constraint has been too severe in the past. But extension of this scheme to allow a class of nonrational S functions, as well as to ''mixed'' nonrational-rational forms, has made the schemes more applicable in actual cases. Essentially then the ''wrong'' pole-zero elements in a rational form of the S function that are needed for a quality fit to any data set, can be structured to form a new ''reference'' function and the inversion potential found again by iteration. Such is the case for the S functions we have found in the analyses of the data sets considered herein.

The 200 MeV p-^{12}C scattering data have been studied previously to specify inversion potentials from use of the (quantal) LF methods [14]. The S functions we have found with this study give very similar results and so no ''new'' inversion potential is shown for this reaction. Therefore, we consider just the ^{16}O-^{16}O and ^{12}C-^{12}C interactions further. The inversion potentials for ^{16}O-^{16}O at 350 MeV and ^{12}C-^{12}C at 288.6 MeV are displayed in Fig. 10 and in the left- and right-hand sides, respectively, and by the solid curves. They are displayed from the radius of 2 fm as that is the smallest radius for which the actual data show sensitivity when the potentials are used in Schrödinger equations with a ''notch test'' procedure used in their solutions. In Fig. 10 the real and imaginary parts of the interactions are given in the top and bottom segments, respectively. Both are net absorptive interactions and are shallow in comparison to the phenomenological and semimicroscopic optical model potentials usually assumed for the heavy ion collisions. But their use in Schrödinger equations leads to relative motion wave functions with asymptotic properties giving the S functions (and so fits to measured data) with which we started. The character of these inversion potentials are not unphysical as smooth, large wavelength oscillatory behavior in local effective interactions may simply be a reflection of true nonlocality in the scattering process. They are different in detail from the result in Ref. [5]. Fully microscopic model calculations of (proton-nucleus) optical interactions [19] also yield effective local interactions with long wavelength oscillations; albeit with much smaller amplitude. Two other inversion potentials for ^{12}C-^{12}C scattering at 288.6 MeV are displayed in Fig. 10. Those results, shown therein by the long- and short-dashed curves, respectively, are the inversion potentials we have obtained with the (eight-pair) fits to the GCV data set and with the optimal four-pair fit to the original data. Clearly the eight-pair (GCV) result is similar to the potential found from inversion of the original data set and the four-pair result is not. The four-pair interaction is overall shorter ranged, more refractive but similarly absorptive to the others.

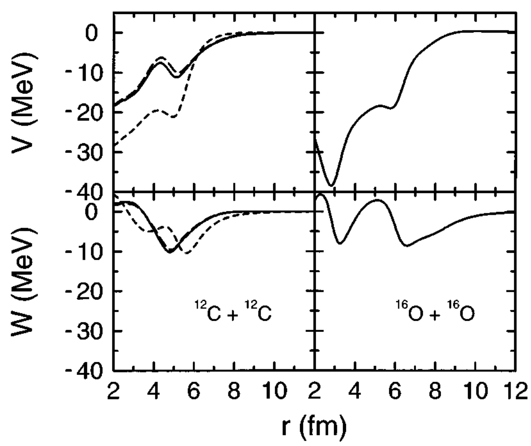

FIG. 10. The real (top) and imaginary (bottom) components of inversion potentials found by LF inversion of original data sets. The results displayed on the left are those found by starting with the S functions found from the eight- and four-pole–zero-pair fits to the 288.6 MeV ^{12}C-^{12}C scattering data (solid and short-dashed curves, respectively) and from that (eight-pole–zero-pair) fit to the associated GCV data set (long-dashed curves). On the right are shown the potentials for ^{16}O-^{16}O scattering at 350 MeV.

VI. WKB ERROR ANALYSIS OF THE POTENTIALS

A full account of the WKB approximation method of error analyses of calculated phase shifts (S functions) and derived quantities has been published [17,18], so only the essential features are given here. We consider first an assessment of errors in specifying the phase shifts. This requires evaluation of the error matrix defined from the covariance of the parameters used to specify those phase shifts. If the parameters collectively are designated by $\mathbf{a}=\{a_n\}$, the error matrix is given by the matrix elements

$$\epsilon_{nm}=\langle\Delta a_n\Delta a_m\rangle=\beta_{nm}^{-1}(\chi^2/F). \qquad (16)$$

There $\Delta a_n = a_n - \hat{a}_n$, where $\{\hat{a}_n\}$ is the set of parameters for which

$$\chi^2/F = \frac{1}{M-4N} \sum_{i=1}^{M} \frac{[\sigma_i - \sigma(\theta_i, \mathbf{a})]^2}{(\Delta\sigma_i)^2} \tag{17}$$

is a minimum. Note that we choose N to be the number of pole-zero pairs, ($\{\alpha_j, \beta_j\}$, $j=1,2,\ldots,N$), so that with four distinct components to each pole-zero pair, the parameter set is a vector of length $4N$. The inverse of the matrix element weighted by the χ^2/F in Eq. (16) is given by

$$\beta_{nm} = (M-4N)\alpha_{nm}, \tag{18}$$

where

$$\alpha_{nm} = \frac{1}{2} \left. \frac{\partial^2(\chi^2/F)}{\partial a_n \partial a_m} \right|_{\hat{a}}. \tag{19}$$

The data set has been assumed to contain M entries, σ_i, each having a statistical error of $\Delta\sigma_i$.

The errors in any specified quantity (S function, potential, etc.) can be obtained from the appropriate covariance which for the case of the LF (WKB) inversion potential gives

$$[\Delta V(r)]^2 = \sum_{n,m=1}^{4N} \left. \frac{\partial V(r)}{\partial a_n} \frac{\partial V(r)}{\partial a_m} \right|_{\hat{a}} \epsilon_{nm}, \tag{20}$$

where

$$\frac{\partial V(r)}{\partial a_n} = \exp[-Q(s)/E] \frac{\partial Q(s)}{\partial a_n}, \quad n=1,2,\ldots,4N \tag{21}$$

when $Q(s)$ is the quasipotential defined by Eq. (8) and $s=\sigma/k$.

The quality of both the ^{16}O-^{16}O and ^{12}C-^{12}C scattering data and of the fits we have found to them allows us to use the theory outlined above to make an (WKB) error analysis of the (WKB) LF inversion potentials. For those radii where the WKB approximation result agrees with the fully quantal inversion interaction then we ascribe the same errors (confidence limits) to the quantal potential.

This approach has been used in the recent past [18] to analyze data from electron-He atom scattering. The results gave ''confidence'' limits for the potentials at each and every radial point and are to be interpreted as follows. Should another potential exist which fits the cross-section data with the same χ^2/F, then there is $\approx$67% probability that it will lie within the confidence bands we show.

In Fig. 11 the WKB and fully quantal inversion potentials are shown for the ^{16}O-^{16}O and ^{12}C-^{12}C scatterings on the right- and left-hand sides. The latter are the results obtained from our (four-pole–zero-pair fit) analyses. In this figure, the solid curves represent the real parts of the (fully quantal inversion) potentials, while the dashed curves denote the associated imaginary parts. The WKB potentials, with associated errors, are plotted for select radii as solid circles; the ''error bars'' being the confidence intervals found for each point. As with the results found previously with the inversion potential from analyses of the 200 MeV proton-^{12}C scattering data

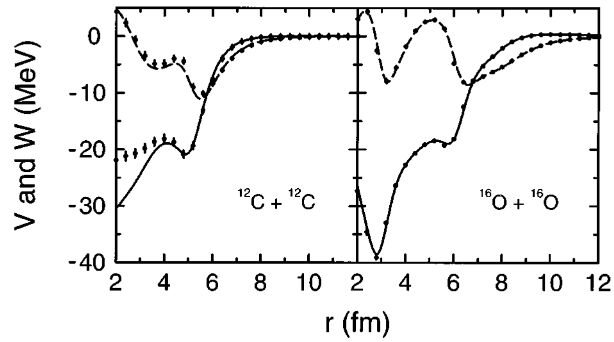

FIG. 11. The inversion potentials for ^{12}C-^{12}C scattering at 288.8 MeV (left panel) and for 350 MeV ^{16}O-^{16}O scattering (right panel) found by the LF full quantal inversion method (the solid curve gives the real part and the dashed curve gives the imaginary part) and by the WKB approximation (solid circles at select scattering angles). The ''error'' bars on the WKB results give the approximate 67% confidence bands described in the text.

[14], in these cases the confidence intervals on the inversion potentials are also of the order of a few percent at most radii. These confidence limits are small at all radii reflecting a very tight band of ($\approx$67%) probability content. Note, however, that for the ^{12}C-^{12}C scattering, the complex WKB method itself becomes inaccurate at about 4 fm.

It is to be stressed that the above results only pertain to the family of rational scattering functions used to fit the experimental data. Ambiguities that may be generated with other classes of potentials are not explicitly considered, and in fact may give confidence levels from error analyses much in excess of those found herein. Conventional optical model approaches should be appraised with these means in future studies to delineate the associated parameter values and the confidence limits one should place upon the resultant potential.

VII. CONCLUSIONS

Analyses of both unknown and known systematic error effects on three differential cross-section data sets have been made. All three data sets used are significant ones insofar as their relevance in theoretical studies of optical model interactions. The effects of unknown systematic errors have been assessed by applying generalized cross validation to the data sets. For those cases with which angular resolution of the data has been given, that form of known systematic error has been considered by a simple data smoothing technique. In the case of p-^{12}C scattering at 200 MeV a statistically significant fit to the data of $\chi^2/F=0.99$ remained virtually unchanged once GCV was applied to the data. We therefore conclude that this data was *a priori* optimally smooth. For the ^{16}O-^{16}O data at 300 MeV a GCV analysis reduced χ^2/F from 10.5 to 7.9, still of low statistical significance. However, an angle smoothing procedure taking into account the quoted finite angular resolution reduced this to $\chi^2/F=0.98$. A subsequent GCV analysis of this angle smoothed data set showed that it was optimally smooth. In the case of ^{12}C-^{12}C at 288.6 MeV, an initially good fit of $\chi^2/F=1.07$ became 0.86 upon application of the GCV procedure, once again indicating the smooth nature of this data in the first place. Angle smoothing gave the large effect of overdetermination. The χ^2/F was reduced to 0.44. The smoothing process thereby allowed us to look for simpler (fewer parameter values) S functions and still retain a statistically significant fit to the data.

The S functions used to fit the scattering data, be it the original, GCV, or angle adjusted set was of the form that could be used in a fixed energy inversion scheme of the Lipperheide-Fiedeldey type. Stable smooth complex interactions were thereby obtained and they demonstrate a characteristic behavior. These local effective interactions are shallow, net weakly absorptive and have long wavelength oscillations. Such behavior has been noted in fully microscopic calculations of 200 MeV proton-carbon scattering potentials although the variations are not so pronounced. The results are stable and given the quality of fit to the data set by each underlying S function, error analyses of the inversion potentials give quite narrow confidence levels at physically important radii. Of course, while another potential with a similar value of χ^2/F has a $\sim$67% probability of lying within the displayed ''error'' bars, it is a potential of the same family (class).

[1] K. Chadan and P. S. Sabatier, *Inverse Problems in Quantum Scattering Theory*, 2nd ed. (Springer, Berlin, 1989).

[2] R. Lipperheide, H. Fiedeldey, and H. Leeb, in *Advanced Methods in the Analysis of Nuclear Scattering Data*, Lecture Notes in Physics Vol. 236, edited by H. C. Krappe and R. Lipperheide (Springer, Berlin, 1985), and references cited therein; H. Leeb, H. Fiedeldey, and R. Lipperheide, Phys. Rev. C **32**, 1223 (1985); S. G. Cooper, M. W. Kermode, and L. J. Allen, J. Phys. G **12**, L291 (1986); R. S. Mackintosh and S. G. Cooper, Nucl. Phys. **A494**, 123 (1989).

[3] E. J. Kujawski, Phys. Rev. C **6**, 709 (1972); **8**, 100 (1973); H. Fiedeldey, R. Lipperheide, K. Naidoo, and S. A. Sofianos, *ibid.* **30**, 434 (1984); K. Naidoo, H. Fiedeldey, S. A. Sofianos, and R. Lipperheide, Nucl. Phys. **A419**, 13 (1984); L. J. Allen, K. Amos, C. Steward, and H. Fiedeldey, Phys. Rev. C **41**, 2021 (1990); L. J. Allen, H. Fiedeldey, S. A. Sofianos, K. Amos, and C. Steward, *ibid.* **44**, 1606 (1991); L. J. Allen, K. Amos, and H. Fiedeldey, J. Phys. G **18**, L179 (1992).

[4] H. Leeb, C. Steward, K. A. Amos, and L. J. Allen, Phys. Rev. C **45**, 2919 (1992).

[5] L. J. Allen, L. Berge, C. Steward, K. Amos, H. Fiedeldey, H. Leeb, R. Lipperheide, and P. Fröbrich, Phys. Lett. B **298**, 36 (1992).

[6] D. R. Lun, X. J. Chen, L. J. Allen, and K. Amos, Phys. Rev. A **49**, 3788 (1994); **50**, 4025 (1994).

[7] C. Steward, H. Fiedeldey, K. Amos, and L. J. Allen, Phys. Rev. C **51**, 836 (1995).

[8] G. R. Satchler, Nucl. Phys. **A574**, 575 (1994).

[9] P. Craven and G. Wahba, Num. Math. **31**, 377 (1979).

[10] G. M. Laslett, J. Am. Stat. Assoc. **89**, 391 (1994).

[11] H. O. Meyer, P. Schwandt, W. W. Jacobs, and J. R. Hall, Phys. Rev. C **27**, 459 (1983).

[12] H. B. Bohlen, E. Stilliaris, B. Gebauer, W. von Oertzen, M. Wilpert, Th. Wilpert, A. Ostrowski, Dao T. Khoa, A. S. Demyanova, and A. A. Ogloblin, Z. Phys. A **346**, 189 (1993).

[13] A. J. Cole, W. D. M. Rae, M. E. Brandan, A. Dacal, B. G. Harvey, R. Legrain, M. J. Murphy, and R. G. Stokstad, ''Elastic Scattering of C12-C12 between 121 and 290 MeV,'' University of California Report LBL 14550, 1982.

[14] L. J. Allen, K. Amos, and P. J. Dortmans, Phys. Rev. C **49**, 2177 (1994).

[15] R. Lipperheide and H. Fiedeldey, Z. Phys. A **286**, 45 (1978); **301**, 81 (1981).

[16] M. J. Brunger *et al.*, J. Phys. B **25**, 1823 (1992).

[17] L. J. Allen, Phys. Rev. A **34**, 2706 (1986).

[18] L. J. Allen and I. E. McCarthy, Phys. Rev. A **36**, 2570 (1987).

[19] L. Rikus, K. Nakano, and H. V. von Geramb, Nucl. Phys. **A414**, 413 (1984); P. J. Dortmans and K. Amos, Phys. Rev. C **49**, 1309 (1994); S. Karataglidis, P. J. Dortmans, K. Amos, and R. de Swiniarski, Phys. Rev. C **52**, 861 (1995).